

# AUTOSIZER: Automatic Sizing of Analog and Mixed-Signal Circuits via Large Language Model (LLM) Agents

**Xi Yu**<sup>1</sup> **Dmitrii Torbunov**<sup>1</sup> **Soumyajit Mandal**<sup>2</sup> **Yihui Ren**<sup>1</sup>

## Abstract

The design of Analog and Mixed-Signal (AMS) integrated circuits remains heavily reliant on expert knowledge, with transistor sizing a major bottleneck due to nonlinear behavior, high-dimensional design spaces, and strict performance constraints. Existing Electronic Design Automation (EDA) methods typically frame sizing as static black-box optimization, resulting in inefficient and less robust solutions. Although Large Language Models (LLMs) exhibit strong reasoning abilities, they are not suited for precise numerical optimization in AMS sizing. To address this gap, we propose AUTOSIZER, a reflective LLM-driven meta-optimization framework that unifies circuit understanding, adaptive search-space construction, and optimization orchestration in a closed loop. It employs a two-loop optimization framework, with an inner loop for circuit sizing and an outer loop that analyzes optimization dynamics and constraints to iteratively refine the search space from simulation feedback. We further introduce AMS-SIZINGBENCH, an open benchmark comprising 24 diverse AMS circuits in SKY130 CMOS technology, designed to evaluate adaptive optimization policies under realistic simulator-based constraints. AUTOSIZER experimentally achieves higher solution quality, faster convergence, and higher success rate across varying circuit difficulties, outperforming both traditional optimization methods and existing LLM-based agents.

## 1. Introduction

The design of Analog and Mixed-Signal (AMS) circuits typically follows a multi stage workflow that begins with

<sup>1</sup>Artificial Intelligence Department, Brookhaven National Laboratory, Upton, NY <sup>2</sup>Instrumentation Department, Brookhaven National Laboratory, Upton, NY 11973 . Correspondence to: Xi Yu <xyu1@bnl.gov>.

topology selection and transistor sizing and then proceeds to layout level steps such as placement routing and verification while optimizing power efficiency maximizing performance and minimizing area to meet target specifications. These multi-stage workflows are complex, requiring time-consuming simulations along with human expertise. Among these stages, circuit sizing is particularly challenging because it involves a high dimensional design space and complex trade offs among multiple performance metrics, where small variations in device parameters can lead to significant and often non linear changes in circuit behavior and overall performance. As a result, automatic circuit sizing has emerged as a crucial problem in electronic design automation (EDA) and has attracted increasing research attention.

Traditional methods formulate the circuit sizing as an optimization problem, such as Bayesian Optimization (BO) (Touloupas et al., 2021; Lyu et al., 2018), Reinforcement Learning (Wang et al., 2020), and genetic algorithms (Cohen et al., 2015). However, these approaches treat the circuit design space as a static black box, ignoring domain-specific analog design expertise and often yielding suboptimal solutions. Recently, LLM-based agents have shown promise in symbolic reasoning and scientific problem solving. Several studies have explored LLMs for automated analog circuit design, focusing on circuit knowledge representation and sizing optimization. EEsizer (Liu & Chitnis, 2025b) directly uses an LLM for both circuit understanding and sizing optimization. Other LLM-agent approaches (Liu et al., 2024; Somayaji & Li, 2025) emphasize improving circuit comprehension through document parsing or structured knowledge bases. LEDRO (Kocher et al., 2025) leverages LLMs to reduce the design search space and improve optimization efficiency, while LLMACD (Xu et al., 2025) incorporates a pre-trained Transistor Behavioral Model (TBM) to enhance design consistency. Despite these advances, most existing agents rely on fixed optimization algorithms and single-stage workflows, in which the LLM interprets the circuit, applies a predetermined optimization strategy, and outputs results without iterative self-reflection or feedback-driven refinement. This limits their ability to adapt the optimization process itself in response to intermediate outcomes, particularly for complex AMS circuits with sparse feasibility regions and competing design objectives.

Table 1. Comparison of LLM-based Agents circuit-sizing methods and benchmark coverage.

Method	Self Reflection	Adaptive Optimization Tools	Search Space construction	Benchmark (Circuit Type & # Num)						
				Amp.	Osc.	SC	Logic/ Comp.	Ref./ Power	Filter	# Num
AmpAgent (Liu et al., 2024)	X	X	X	✓	X	X	X	X	X	7
ADO-LLM (Yin et al., 2024)	X	X	X	✓	X	X	✓	X	X	2
LLM-USO (Somayaji & Li, 2025)	X	X	X	✓	X	X	✓	✓	X	4
LLMACD (Xu et al., 2025)	X	X	X	✓	X	X	X	X	X	2
LEDRO (Kocher et al., 2025)	✓	X	✓	✓	X	X	X	X	X	22
EEsizer (Liu & Chitnis, 2025b)	✓	X	X	✓	✓	X	✓	X	X	6
AutoSizer	✓	✓	✓	✓	✓	✓	✓	✓	✓	24

To address this gap, we propose AUTOSIZER, a reflective meta-optimization framework based on multi-agent LLMs for automatic sizing optimization of analog and mixed-signal circuits. AUTOSIZER integrates circuit understanding, adaptive search-space construction, and optimization algorithm orchestration into a unified, closed-loop workflow with an evaluation agent, enabling efficient and robust exploration of high-dimensional design spaces. Starting from user specifications and circuit netlists, an LLM-based circuit understanding agent analyzes the circuit topology to identify key design variables and infer their functional roles and performance sensitivities. Based on this analysis, a search-space decision agent prioritizes the identified variables and dynamically assigns feasible ranges, enabling the framework to focus optimization effort on the most impactful parameters. Sizing optimization is carried out in a **two-loop optimization framework**. The inner loop performs **numerical circuit sizing** using a configurable optimization engine that supports multiple algorithms, such as Latin Hypercube Sampling (LHS), genetic algorithms, Bayesian Optimization (BO), and related methods, and evaluates simulation results against user-defined specifications. The outer loop performs **reflective search-space evaluation and refinement** by analyzing optimization history, convergence behavior, and constraint satisfaction. Based on this feedback, the framework adaptively revises variable priorities, tightens or expands parameter ranges, and updates circuit understanding, enabling progressive and data-efficient refinement of the design space across iterations.

To support systematic and reproducible evaluation of adaptive sizing strategies, we introduce AMS-SIZINGBENCH, a new benchmark suite for analog and mixed-signal circuit sizing optimization built entirely on the open-source SKY130 CMOS technology. The benchmark comprises of 24 representative analog and mixed-signal circuits, spanning a wide range of design complexities from basic building blocks to advanced functional modules, and is carefully organized to provide a fully open and standardized sizing environment. Each benchmark instance includes the SKY130-based cir-

cuit netlist, a clearly defined set of sizing variables and optimization constraints, and a complete simulation workflow for performance evaluation. AMS-SIZINGBENCH thus provides a fully open and standardized testbed for evaluating adaptive optimization policies and facilitates fair comparison, extensibility, and reuse in AMS sizing research.

Our contributions can be summarized as follows:

- **An LLM-driven two-loop multi-agent framework for analog and mixed-signal sizing.** We propose AUTOSIZER, a multi-agent LLM framework that formulates AMS sizing as a meta-optimization problem, integrating circuit understanding, adaptive search-space construction, and optimization algorithm orchestration into a unified closed-loop workflow. The framework combines an inner sizing optimization loop that supports multiple optimization algorithms with an outer search-space refinement loop that analyzes optimization history, convergence behavior, and variable impact, enabling adaptive revision of variable priorities and parameter ranges for efficient exploration of high-dimensional design spaces.
- **AMS-SIZINGBENCH: an open benchmark for AMS circuit sizing systematic evaluation.** We present AMS-SIZINGBENCH, a fully open-source benchmark suite built on the SKY130 CMOS technology, comprising 24 representative analog and mixed-signal circuits spanning a wide range of design complexities. Each benchmark instance includes a standardized circuit netlist, clearly defined sizing variables and constraints, and a complete simulation and evaluation workflow, enabling reproducible evaluation and fair comparison of automated sizing methods.
- **Comprehensive experimental evaluation and performance gains.** We conduct extensive experiments on AMS-SIZINGBENCH and show that AUTOSIZER consistently outperforms both traditional optimization methods and existing LLM-based agents in terms of

convergence speed, solution quality, and robustness across diverse circuit types.

## 2. Related Work

Automated sizing of AMS circuits has been a long-standing pursuit in the EDA community, evolving from manual heuristics to simulation-driven optimization and emerging LLM-based agent workflows.

### 2.1. Traditional Circuit Sizing Methods

Traditional circuit sizing methods formulate design as a static black-box optimization problem, obtaining performance metrics through repeated simulations. Early approaches use general-purpose algorithms like simulated annealing and genetic algorithms (Wolfe & Vemuri, 2003; Pessoa et al., 2018), which require tens of thousands of simulations and lack mechanisms for adapting the search space or transferring knowledge across runs. Bayesian optimization (BO) improves sample efficiency using surrogate models (Lyu et al., 2018; Liu et al., 2014; Shahriari et al., 2015), but still relies on fixed parameter spaces and predefined acquisition strategies, and struggles as dimensionality increases. More recently, reinforcement learning (RL) methods (Wang et al., 2018; Settaluri et al., 2020; Yang et al., 2021) demonstrate improved scalability and transfer learning (Zhang et al., 2023; Ahmadzadeh et al., 2025b), yet still require hundreds of computationally expensive simulations and yield opaque, task-specific policies, limiting interpretability and hindering industrial adoption.

### 2.2. LLM Agents

Recent advances in large language models have enabled agent-based systems that move beyond passive text generation toward autonomous, goal-oriented behavior. These LLM agents leverage structured planning, tool interaction, and iterative feedback loops to decompose tasks and refine solutions (Yao et al., 2022; Chen et al., 2024). Many frameworks incorporate memory mechanisms and self-reflective reasoning to accumulate experience and adapt strategies over time. They have been successfully applied across diverse domains including software engineering (Jimenez et al., 2023; Wang et al., 2024), robotics (Brohan et al., 2023; Black et al., 2024), data science (Guo et al., 2024; Hong et al., 2025), and scientific research (Yamada et al., 2025; Baek et al., 2025). In electronic design automation, recent works explore LLM-based approaches for analog circuit design: AnalogXpert (Lai et al., 2025) automates topology synthesis, EEschematic (Liu & Chitnis, 2025a) generates schematics via multimodal agents, AnalogCoder-Pro (Lai et al., 2025) unifies circuit generation and optimization, and SimuGen (Ren et al., 2025) constructs block diagram-based simulation models through multi-modal agents.

### 2.3. LLM-based Agents for Circuit Sizing

Recent work explores using LLMs as autonomous agents for analog circuit sizing. Unlike black-box optimization methods, LLM-based approaches leverage language models to reason about circuit structure, interpret simulation feedback, and guide optimization.. AmpAgent (Liu et al., 2024) retrieves the amplifier-specific knowledge from essays and guides the LLM to optimize the circuit sizing. LLM-USO (Somayaji & Li, 2025) constructs a graph knowledge space and leverage it for the next circuit design. LL-MACD (Xu et al., 2025) generates Transistor Behavioral Circuit Representations (TBCRs) that meet performance targets using knowledge-embedded prompts. LEDRO (Kochar et al., 2025) utilized LLMs alongside fixed optimization techniques to iteratively refine the design space for analog circuit sizing. AnaFlow (Ahmadzadeh et al., 2025a) leverages both reasoning sizing and optimizer sizing. However, existing LLM-based sizing agents rely on either fixed search spaces or fixed optimization algorithms with predetermined configurations, often validated on a single circuit class (e.g., amplifiers). This rigidity limits scalability across diverse designs. AutoSizer addresses these limitations by formulating circuit sizing as a reflective meta-optimization problem, dynamically refining search spaces and orchestrating multiple optimization algorithms based on intermediate optimization dynamics. We evaluate AutoSizer on 24 diverse AMS circuit topologies based on SKY130 CMOS technology, including OTAs, oscillators, voltage references, filters, and voltage regulators, demonstrating robust performance across varied circuit types and specifications.

## 3. Method

### 3.1. Problem Formulation

We formulate AMS circuit sizing as a simulation-driven constrained optimization problem. Let  $\mathbf{x} \in \mathcal{X}$  denote the vector of sizing parameters and  $\mathbf{y} = [y_1, \dots, y_m] = f(\mathbf{x})$  denote the corresponding performance metrics obtained from simulation. A scalar figure of merit (FoM) is defined to capture the trade-off between metrics to be maximized and minimized:

$$\text{FoM}(\mathbf{y}) = \frac{\prod_{i \in \mathcal{D}} \tilde{y}_i}{\prod_{j \in \mathcal{M}} \tilde{y}_j}, \quad (1)$$

where  $\mathcal{D}$  and  $\mathcal{M}$  denote the sets of metrics to be maximized and minimized, respectively, and  $\tilde{y}_i = y_i / y_{i,\text{spec}}$  are normalized with respect to their specification targets  $y_{i,\text{spec}}$ . This normalization ensures FoM values are dimensionless and comparable across circuits with different performance scales. A design is feasible when  $\tilde{y}_i \geq 1$  for all  $i \in \mathcal{D}$  and  $\tilde{y}_j \leq 1$  for all  $j \in \mathcal{M}$ . The sizing task is expressed as:

$$\max_{\mathbf{x} \in \mathcal{X}} \text{FoM}(f(\mathbf{x})) \quad \text{s.t.} \quad \tilde{y}_i \geq 1 \quad \forall i \in \mathcal{D}, \quad \tilde{y}_j \leq 1 \quad \forall j \in \mathcal{M} \quad (2)$$

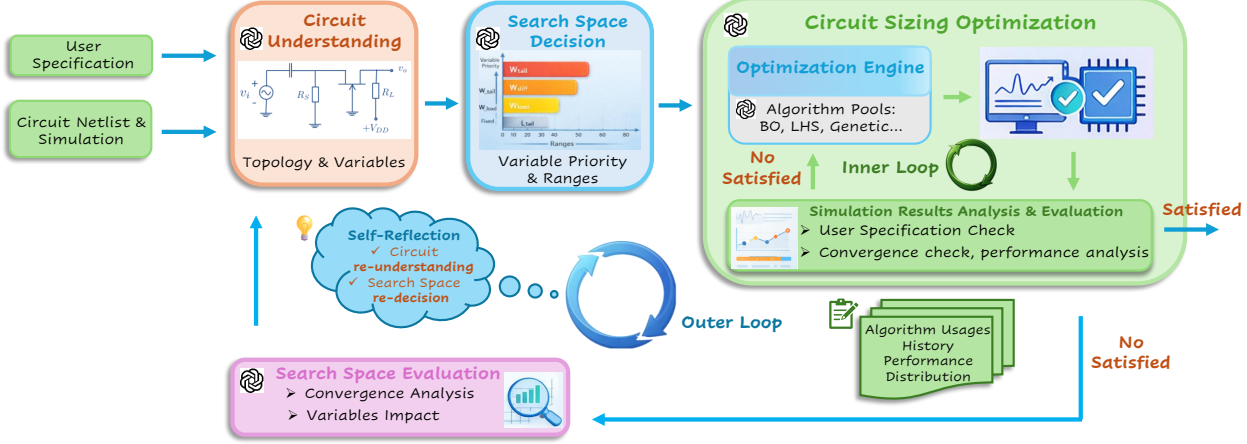


Figure 1. AutoSizer workflow. The framework combines LLM-based circuit understanding with an inner loop that sequentially selects, configures, and applies multiple sizing algorithms and an outer loop that adaptively refines the search space, forming a two-loop closed-loop architecture that enables iterative refinement of variable priorities and parameter ranges based on optimization feedback.

### 3.2. Overview of the AutoSizer Framework

AutoSizer is a multi-agent, LLM-driven framework designed for reflective automatic sizing optimization of AMS circuits. Given user specifications and a circuit netlist, AutoSizer integrates circuit understanding, adaptive search-space construction, and simulation-driven optimization into a unified, closed-loop workflow. Multiple specialized agents collaborate to iteratively refine design decisions using simulation feedback.

As illustrated in Fig. 1, AutoSizer adopts a two-loop optimization architecture. The inner loop optimizes device sizes by invoking a configurable optimization engine and evaluating candidate designs through circuit simulation. The outer loop analyzes optimization outcomes, including convergence behavior and performance distributions, to evaluate optimization effectiveness and constraint satisfaction under the current formulation. Based on this analysis, the framework revises the optimization problem, updating variable priorities, parameter ranges, and circuit understanding through self-reflection, enabling progressive and data-efficient exploration of high-dimensional design spaces.

### 3.3. LLM-Based Circuit Understanding

The purpose of the circuit understanding module is to extract high-level structural and functional knowledge from circuit netlists to guide sizing optimization. Given a circuit netlist and user specifications as input, the LLM produces a structured summary of the circuit topology, key sizing variables, and their qualitative impact on performance metrics.

The model analyzes circuit connectivity, signal paths, and biasing structures to identify major functional blocks, and

maps optimization variables to the corresponding circuit components (See circuit understanding prompt in Appendix B.1). Based on this analysis, it estimates the relative influence of sizing variables on key metrics and identifies fundamental trade-offs.

As can be seen in Figure 2, circuit understanding agent provides an interpretable abstraction of the design space and serves as an explicit input to reflective optimization, directly informing the adaptive search-space construction stage by prioritizing impactful variables and guiding range selection.

#### LLM-Based Circuit Understanding Output

**Circuit Topology:** Telescopic operational transconductance amplifier (OTA) with an NMOS differential input pair, cascaded NMOS and PMOS stages, and PMOS current-mirror loads.

**Key Sizing Variables:**  $W_{\text{diff}}$  (input differential pair),  $W_{\text{casc}}$  (cascode devices),  $W_{\text{tail}}$  (tail current source),  $W_{\text{load}}$  (PMOS load devices).

**Performance Sensitivity:** DC gain is primarily influenced by  $W_{\text{diff}}$  and  $W_{\text{casc}}$ . UGBW is dominated by  $W_{\text{diff}}$ , with secondary dependence on current-scaling variables. Power consumption is mainly controlled by  $W_{\text{tail}}$  and  $W_{\text{load}}$ .

**Key Trade-offs:** Improving gain and bandwidth increases power consumption and parasitic capacitance, requiring careful balance for FoM optimization.

Figure 2. LLM-generated circuit understanding for the telescopic OTA, including topology analysis, key sizing variables, performance sensitivities, and design trade-offs.

### 3.4. Adaptive Search-Space Construction

The adaptive search-space construction module aims to reduce optimization complexity by focusing computational effort on the most impactful design parameters. Its input consists of the structured circuit understanding output and optimization dynamics and feasibility feedback from previous iterations, and its output is a dynamically defined

search space with prioritized variables and feasible parameter ranges.

Directly optimizing over all possible sizing variables with wide parameter ranges leads to prohibitively large search spaces and poor sample efficiency. In practice, only a subset of variables significantly influences circuit performance, and their effective operating ranges are often much narrower than the full technology limits. Inspired by common analog design practice, AutoSizer adopts a progressive, feedback-driven search-space expansion strategy: it begins with a compact search space defined by a small set of high-impact variables and conservative ranges (See Figure 3), and incrementally expands the search space only when optimization outcomes indicate infeasibility or stagnation.

#### First-Round Adaptive Search-Space Construction

**Optimization Target:** Maximize DC gain and unity-gain bandwidth (UGBW) while minimizing power consumption.

**Variable Prioritization:**  $W_{\text{diff}}$  is identified as the most critical variable due to its direct control of input transconductance, which dominates both gain and UGBW.  $W_{\text{tail}}$  and  $W_{\text{load}}$  are ranked next, as they scale bias current and govern the primary power–performance trade-off.  $W_{\text{casc}}$  is treated as a secondary knob that mainly affects gain through output resistance.

**Active Variables and Ranges:**  $W_{\text{diff}} \in \{0.84, 1.26, 1.68, 2.10, 2.52\}$ ,  $W_{\text{tail}} \in \{0.84, 1.47, 2.10, 2.52\}$ ,  $W_{\text{load}} \in \{0.84, 1.47, 2.10, 2.52\}$ . These ranges are chosen to sparsely yet effectively explore performance scaling and the FoM trade-off.

**Fixed Variable:**  $W_{\text{casc}}$  is fixed at 1.89 to reduce search dimensionality while preserving high output resistance for adequate DC gain.

**Search-Space Reduction:** The original full space of  $9^4 = 6561$  combinations is reduced to  $5 \times 4 \times 4 = 80$  combinations, achieving an  $\sim 82 \times$  reduction while maintaining coverage of the dominant design trade-offs.

Figure 3. LLM-generated adaptive search space configuration for the first optimization round, showing variable prioritization, range selection, and dimensionality reduction strategy.

This reduces unnecessary exploration in early stages, focusing effort on promising regions. Upon stagnation or infeasibility, AutoSizer systematically reformulates the problem by unfixing variables or expanding ranges.

#### 3.5. Two-Loop Optimization Framework

AutoSizer adopts a two-loop optimization framework that separates numerical parameter search from adaptive formulation of the optimization problem. The inner loop is responsible for optimizing sizing parameters within a fixed search space, while the outer loop evaluates the effectiveness of the current search space and revises it when necessary.

In the inner loop, AUTOSIZER adaptively selects and configures optimization algorithms from a predefined algorithm pool (See Algorithm Orchestration Prompt in Appendix B.3) based on the current optimization stage, available simulation history, and search-space characteristics determined by the LLM-based search-space decision agent. Candidate designs are evaluated via circuit simulation and scored us-

ing the specifications and FoM, with results shared across algorithms. The inner loop terminates upon convergence or budget exhaustion.

The outer loop monitors optimization outcomes produced by the inner loop, including feasibility status, convergence behavior, and performance trends. If the inner loop fails to identify feasible solutions or exhibits stagnation, the outer loop adaptively revises the optimization problem by adjusting parameter ranges, activating additional variables, or updating variable priorities. This separation of responsibilities enables efficient exploration in early stages while preserving robustness against suboptimal initial search-space assumptions. The complete two-loop optimization procedure is formally described in Algorithm 1.

---

#### Algorithm 1 Two-Loop Optimization Framework

**Require:** Circuit netlist  $\mathcal{N}$ , user specifications  $\mathcal{S}$ , initial search space  $\mathcal{X}_0$

**Ensure:** Optimized sizing parameters  $\mathbf{x}^*$

```

1: Initialize search space decision  $\mathcal{X} \leftarrow \mathcal{X}_0$ 
2: Initialize optimization history  $\mathcal{H} \leftarrow \emptyset$ 
3: while termination condition not met do
4:   Inner Loop: Algorithm Selection & Execution
5:   Select optimization algorithm
6:   Run optimizer  $\mathcal{A}_k(\theta_k)$  within current search space
 $\mathcal{X}$  to generate candidate search samples
7:   for each candidate  $\mathbf{x}$  do
8:     Simulate circuit and evaluate performance
9:     Update optimization history  $\mathcal{H}$ 
10:  end for
11:  Outer Loop: Search-Space Refinement
12:  if feasible solution found then
13:    break
14:  end if
15:  if convergence stagnates or constraints violated then
16:    Analyze  $\mathcal{H}$  to identify limiting variables
17:    Update search space  $\mathcal{X}$  by adjusting ranges or
activating new variables
18:  end if
19: end while
20: return Best feasible solution  $\mathbf{x}^*$ 

```

---

#### 3.6. Evaluation and Feedback Mechanism

The evaluation and feedback mechanism in AUTOSIZER operates at two levels, supporting both inner-loop optimization control and outer-loop search-space refinement, as illustrated in Figure 4. Its role is to assess optimization progress, diagnose bottlenecks, and provide structured feedback for adaptive decision-making across iterations.

**Inner-loop evaluation** assesses the effectiveness of the current sizing optimization strategy and guides algorithm selection and configuration. After each iteration, AutoSizer

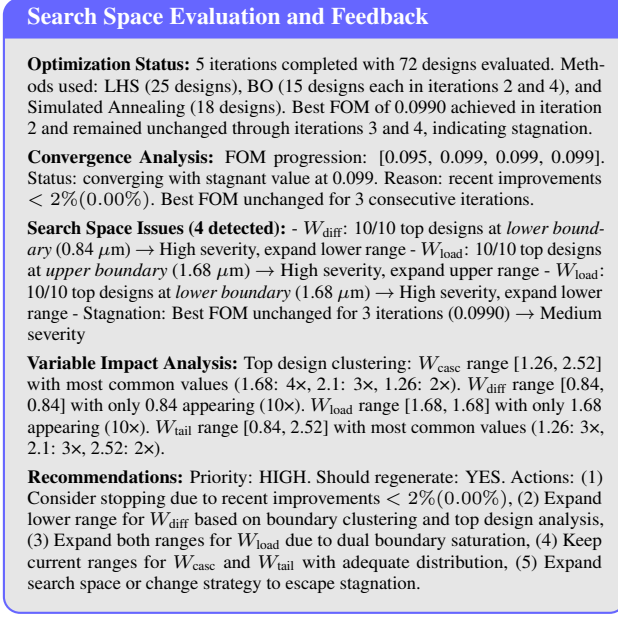


Figure 4. Search space evaluation and feedback from AutoSizer agent after inner loop finished with 4 optimization iterations.

summarizes optimization outcomes using statistics such as FoM improvement, feasibility status, and parameter diversity. Based on these signals, the framework dynamically selects and configures optimization algorithms to balance exploration and exploitation, and determines termination when specifications are satisfied or convergence is detected. **Outer-loop evaluation** assesses whether the current search space is sufficient to meet design objectives and guides high-level adaptation when necessary. It aggregates inner-loop optimization outcomes across iterations, including feasibility trends, FoM improvement trajectories, performance distributions, and parameter concentration patterns. By analyzing these signals, the outer loop identifies cases where optimization progress saturates within the current parameter bounds or where high-performing solutions consistently occur near search-space edges. In such cases, the search space is refined by adjusting parameter ranges, re-prioritizing variables, or activating previously fixed variables. By decoupling evaluation at the optimization and search-space levels, AutoSizer ensures that both numerical optimization decisions and higher-level design-space refinement utilize quantitative, simulation-based evidence.

## 4. Experiments

### 4.1. Experimental Setup

**Benchmark and Evaluation.** We evaluate on AMS-SIZINGBENCH, an open SKY130-based benchmark suite consisting of 24 analog and mixed-signal circuits, including logic blocks, OTAs, oscillators, switched-capacitor circuits,

voltage references, and voltage regulators, with predefined Easy, Medium, and Hard difficulty splits. Additional details of the AMS-SIZINGBENCH benchmark, including circuit descriptions, input signals, specifications, simulations, and configuration formats, are provided in Appendix A. Each circuit sizing task is a simulation-driven constrained optimization problem maximizing a figure-of-merit (FoM). Circuit performance evaluation uses Ngspice (Vogt et al., 2021) for electrical simulation with the SKY130 PDK.

**Baselines.** We compare AutoSizer against two categories of circuit sizing methods. *Traditional optimization algorithms* include Genetic Algorithm (GA) (Taherzadeh-Sani et al., 2003), Bayesian Optimization (BO), and Trust Region Bayesian Optimization (TuRBO) (Eriksson et al., 2019), representing evolutionary, surrogate-based, and trust region approaches respectively. *LLM-based agent methods* include ADO-LLM (Yin et al., 2024), LEDRO (Kocher et al., 2025), and EE-Sizer (Liu & Chitnis, 2025b). The remaining three baselines are not included due to reproducibility considerations. AmpAgent, LLM-USO, and LLM-ACD are not open-source, and the available descriptions in their respective papers lack sufficient detail for reliable reproduction.

**Implementation Details.** AutoSizer is powered by Gemini-2.5-Flash with a temperature of 0.4,  $\text{top-}p = 0.85$ ,  $\text{top-}k = 20$ , and a maximum of 8192 output tokens. To isolate algorithmic contributions from LLM backend differences, we re-implemented LEDRO, ADO-LLM, and EE-Sizer using the same Gemini-2.5-Flash configuration and a unified 300-sample budget as AutoSizer. We maintain the core algorithmic logic of each method while standardizing the LLM interface and sample accounting, which enables fair comparison of optimization strategies independent of LLM-specific capabilities. Traditional baselines include: (i) a genetic algorithm (GA) with population size 20, crossover rate 0.8, mutation rate 0.1, tournament selection, and elitism; (ii) Bayesian optimization (BO) using a Gaussian Process with a Matérn kernel ( $\nu = 2.5$ ) and UCB acquisition ( $\beta = 2.0$ ), initialized with 10 random samples; and (iii) TuRBO with adaptive trust regions initialized at 0.8 and scaled by  $2 \times / 0.5 \times$  on success/failure. All methods use a total budget of searching 300 samples. EE-Sizer runs 10 iterations with 30 LLM-generated candidates per iteration. AutoSizer uses up to three outer-loop iterations with 100 samples per inner loop, dynamically allocating samples across multiple optimization algorithms within each inner loop.

### 4.2. Overall Performance on AMS-SIZINGBENCH

Table 2 reports average three trials experimental results on the AMS-SIZINGBENCH across three difficulty levels. Performance is evaluated using Figure of Merit (FOM), number of evaluations to best solution (Evals), runtime per trial

(Time), and success rate (SR), defined as the percentage of trials that meet user specifications. On the Hard benchmark, baseline LLM-based agents significantly outperform traditional optimization methods, achieving higher success rates with substantially fewer search samples. As circuit complexity increases, the design space becomes highly nonlinear and constrained; in this regime, LLM-based agents can leverage embedded circuit knowledge to guide the search more efficiently, resulting in improved robustness and efficiency. In contrast, traditional methods suffer from degraded performance and lower success rates. For the Easy and Medium benchmarks, baseline LLM-based agents exhibit comparable performance to traditional methods, indicating that when the search space is relatively simple, conventional optimization techniques remain competitive. Among the LLM-based baselines, ADO-LLM performs worse due to the absence of a self-reflection mechanism, which prevents it from guaranteeing that the LLM-generated search directions remain valid, leading to suboptimal exploration. EE-Sizer relies solely on the LLM without an explicit optimization algorithm; consequently, it requires more LLM interactions per iteration and explores a larger search space, resulting in increased runtime. LEDRO adopts a fixed optimization configuration, which limits its flexibility and reduces effectiveness, particularly for complex circuits. In contrast, our method leverages adaptive optimization strategies guided by LLM reasoning, enabling more efficient exploration of the design space and consistently superior performance across all difficulty levels, especially on complex circuit sizing tasks.

### 4.3. Ablation Studies

We systematically disable individual modules, Circuit Understanding (CU), Initial Search Space Decision (SSD), Optimization Engine (OE), and Self-Reflection Loop (SRL), and measure impact on 5 circuits (1 easy, 2 medium, 2 hard) with 3 trials each. Table 3 shows averaged results, revealing component importance and interdependencies.

**Component ranking.** Ablation results establish clear hierarchy: SRL (-39.4% FOM) > OE (-23.9%) > CU (-19.2%). This ranking demonstrates that *iterative refinement* (SRL) is more critical than *getting initial decisions right* (CU), and *how you search* (OE) matters more than *where you search* (CU). Efficient exploration can partially compensate for suboptimal spaces, but optimal spaces cannot compensate for inefficient exploration. **SRL enables recovery from mistakes.** Removing SRL causes 80% success rate drop (100% → 20%) and 39.4% FOM loss. Single-cycle optimization is fragile because initial search space decisions may be incorrect and cannot be corrected. SRL’s iterative refinement, early cycles explore broadly, later cycles exploit refined regions which is essential for robust convergence across diverse circuits. **OE improves sample efficiency.** Without

OE, fixed Bayesian Optimization requires 37.5% more evaluations and 2x longer runtime, achieving only 50% success rate. Adaptive algorithm selection matches algorithms to optimization phases reducing wasted evaluations. **CU and SSD are interdependent.** A counterintuitive result: w/o CU degrades to 28.65 FOM (-19.2%), but w/o CU & SSD improves to 33.43 FOM (-5.7%). This demonstrates that **search space reduction requires accurate circuit understanding.** Without CU insights, SSD uses naming heuristics that make incorrect assumptions, constraining search to suboptimal subspaces or fixing critical variables. The full space (w/o CU & SSD) avoids these errors, outperforming misguided reduction by 16.7% despite requiring 13.9% more evaluations. **Synergistic design.** Components work synergistically to achieve best performance. Removing any component breaks this synergy, with poorly informed reduction worse than no reduction, validating the necessity of LLM-based circuit analysis.

### 4.4. Analysis and Discussion

To understand AutoSizer’s optimization dynamics, we visualize search space evolution, algorithm selection and converge patterns within the inner loop, and average self-reflection circle of ring oscillator, and search space reduction across circuit difficulties, illustrated in Figure 5.

The search space evolution demonstrates strategic progressive refinement. Figure 5a shows how variable ranges adapt across three Self-Reflection Loop cycles starting from the Original full search space (blue). Loop 1 (orange) aggressively reduces the space by fixing several variables ( $W_{\text{nmos}1}$ ,  $W_{\text{pmos}2}$ ,  $W_{\text{nmos}2}$ ) at specific values while keeping others active ( $W_{\text{pmos}0}$ ,  $W_{\text{nmos}0}$ ,  $L_{\text{inv}}$ ). Loop 2 (green) refines further but strategically re-expands certain dimensions ( $W_{\text{pmos}1}$ ,  $W_{\text{nmos}1}$ ) that proved important in Loop 1, demonstrating adaptive recovery from over-aggressive reduction. Loop 3 (red) achieves the most focused search space, concentrating exploration on the critical subset of variables ( $W_{\text{nmos}0}$ ,  $W_{\text{pmos}2}$ ,  $W_{\text{nmos}2}$ ) while fixing others. The non-monotonic refinement pattern where some dimensions shrink while others expand, confirming that space adaptation is data-driven based on observed performance rather than following pre-determined monotonic reduction, enabling the system to recover from suboptimal early decisions.

The convergence curves show consistent improvement across refinement cycles. Figure 5b demonstrates that each outer loop starts with higher FOM than the previous cycle’s starting point and achieves progressively better final performance. Within each cycle, the system saves optimization history at every iteration, enabling the LLM to make informed decisions about algorithm selection and configuration based on observed convergence patterns. This pattern where later cycles both start better and converge faster val-

Table 2. Experimental results on AMS-SIZINGBENCH. FOM, Eval, Time (s), and SR% denote *Figure of Merit*, *Evaluations to best*, *time per trial*, and *% of trials meeting user specs*, respectively. **Bold** indicates the best result and underline indicates the second best result.

Methods	Easy				Medium				Hard			
	FOM↑	Evals↓	Time (s)↓	SR%↑	FOM↑	Evals↓	Time (s)↓	SR%↑	FOM↑	Evals↓	Time (s)↓	SR%↑
<b>Traditional Method</b>												
Genetic	30.2 ± 1.6	110.5 ± 42.9	515.6 ± 28.5	93.3%	30.7 ± 1.8	193.7 ± 47.9	1638.6 ± 18.4	73.3%	45.3 ± 3.5	165.6 ± 49.2	1689.2 ± 65.1	50.0%
BO	24.1 ± 4.0	84.0 ± 21.4	415.0 ± 55.8	80.0%	31.2 ± 3.6	153.6 ± 59.8	1492.5 ± 48.7	73.3%	46.2 ± 2.3	151.3 ± 51.2	1875.1 ± 73.5	50.0%
TuRBO	15.8 ± 3.9	20.6 ± 6.9	141.0 ± 15.6	39.8%	27.4 ± 4.3	75.7 ± 25.1	1250.2 ± 18.3	39.8%	36.7 ± 12.7	107.2 ± 19.1	2105.2 ± 42.7	25.0%
<b>LLM-based Agent</b>												
ADO-LLM	25.2 ± 3.5	87.2 ± 11.5	527.2 ± 20.8	80.0%	29.2 ± 2.7	148.5 ± 23.5	1328.6 ± 25.8	80.0%	47.3 ± 9.1	162.3 ± 42.3	1278.5 ± 68.5	41.0%
LEDRO	31.3 ± 8.7	65.6 ± 13.4	385.6 ± 15.5	100%	31.6 ± 5.6	142.5 ± 32.5	1150.7 ± 25.4	80.0%	50.5 ± 8.5	140.8 ± 23.2	1350.8 ± 62.5	80.0%
EE-Sizer	30.3 ± 9.8	95.3 ± 21.8	756.2 ± 34.2	100%	30.5 ± 5.4	165.2 ± 37.4	1485.3 ± 37.5	80.0%	49.6 ± 11.5	170.8 ± 20.5	1872.6 ± 54.6	56.4%
<b>AUTOSIZER</b>	<b>33.4 ± 9.2</b>	<u>57.8 ± 12.2</u>	<u>362.6 ± 16.6</u>	<b>100%</b>	<b>33.2 ± 2.8</b>	<u>130.9 ± 38.2</u>	<b>1049.8 ± 16.6</b>	<b>100%</b>	<b>60.2 ± 3.4</b>	<u>128.9 ± 23.0</u>	<b>1152.6 ± 48.1</b>	<b>100%</b>

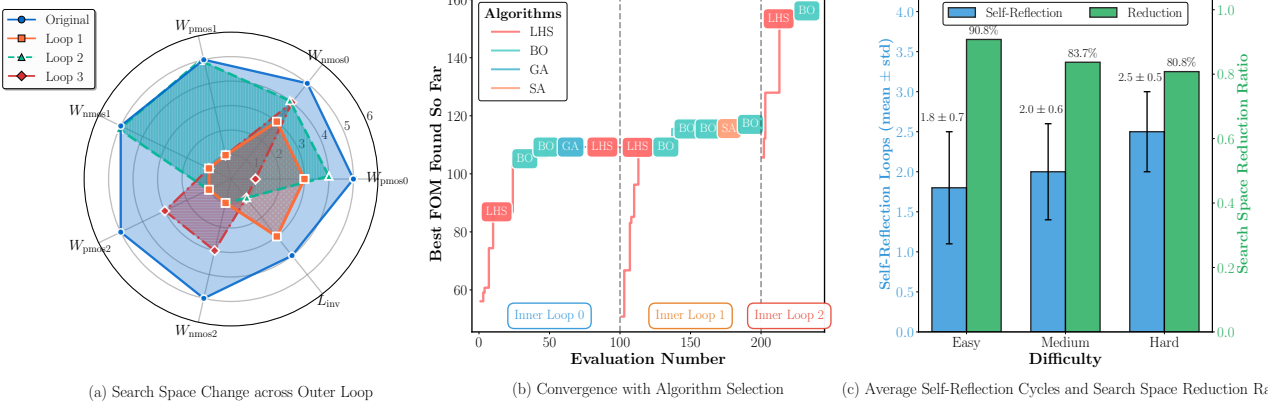


Figure 5. AutoSizer’s optimization dynamics across three outer loops. (a) Progressive search space changes showing active variables (multiple values) and fixed variables (single value) in each outer loop of the ring oscillator. (b) Convergence trajectory with adaptive algorithm selection (LHS, BO, GA, SA) across inner loop of the ring oscillator. (c) Self-reflection loops and search space reduction ratios across circuit difficulties.

Table 3. Ablation study of AutoSizer on 5 representative circuits (1 easy, 2 medium, and 2 hard). CU: Circuit Understanding. SSD: Initial Search Space. OE: Optimization Engine (LLM with algorithm pool). SRL: Self-Reflection Loop.

Methods	Components				Metrics			
	CU	SSD	OE	SRL	FOM↑	Evals↓	Time↓	SR%↑
AutoSizer (Full)	✓	✓	✓	✓	<b>35.47</b>	<b>127.5</b>	925.8	<b>100%</b>
w/o CU	✗	✓	✓	✓	28.65	137.5	1206.4	73.4%
w/o CU & SSD	✗	✗	✓	✓	33.43	145.2	1053.8	86.8%
w/o OE	✓	✓	✗	✓	27.00	175.4	1881.4	50.0%
w/o SRL	✓	✓	✓	✗	25.32	150.9	956.8	50.0%
w/o CU & SSD & SRL	✗	✗	✓	✗	21.51	136.5	857.6	20.0%

icates that Self-Reflection Loop’s search space decisions are correct: refined spaces eliminate unpromising regions, enabling each cycle to build upon previous insights rather than restarting from scratch.

Circuit difficulty affects iteration requirements but not reduction effectiveness. Figure 5c shows that harder circuits require more self-reflection outer loop due to increased specification complexity and sparser feasible design regions. These additional iterations are needed to progressively refine the search space through variable unfixing and range expand-

sion when initial configurations prove insufficient. However, search space reduction remains consistent across all difficulty levels, demonstrating that LLM-based circuit analysis effectively identifies high-impact variables regardless of topology complexity.

## 5. Conclusion

In this work, we propose AUTOSIZER, a reflective meta-optimization framework based on LLMs-based agents for automatic analog and mixed-signal circuit sizing. Additionally, we introduce AMS-SIZINGBENCH, a comprehensive open-source benchmark for evaluating LLM-based agents on analog and mixed-signal circuit sizing that includes SKY130-based circuit netlists, a well-defined set of sizing variables, and a complete simulation workflow for performance evaluation. Comprehensive experiments on the proposed AMS-SIZINGBENCH demonstrate that AUTOSIZER consistently outperforms prior methods in both success rate and figure of merit, particularly on hard, constraint-tight designs. We hope that AUTOSIZER and AMS-SIZINGBENCH provide a foundation for future research in reliable, scalable LLM-driven AMS circuit design automation.

## Impact Statement

This paper presents work whose goal is to advance the fields of Electronic Design Automation and Machine Learning through automated analog circuit design. We note that our framework is designed to augment rather than replace human circuit designers, with interpretable LLM-generated reasoning serving as an educational and verification tool. Users should validate AutoSizer-generated designs through standard verification flows before fabrication. The release of AMS-SizingBench as an open-source benchmark promotes reproducibility and accessibility in circuit optimization research, supporting both academic study and practical deployment of AI-assisted design automation.

## References

Ahmazadeh, M., Chen, K., and Gielen, G. Anaflow: Agentic llm-based workflow for reasoning-driven explainable and sample-efficient analog circuit sizing. In *2025 IEEE/ACM International Conference On Computer Aided Design (ICCAD)*, pp. 1–7. IEEE, 2025a.

Ahmazadeh, M., Lappas, J., Wehn, N., and Gielen, G. Anacraft: Duel-play probabilistic-model-based reinforcement learning for sample-efficient pvt-robust analog circuit sizing optimization. *IEEE Transactions on Computer-Aided Design of Integrated Circuits and Systems*, 2025b.

Baek, J., Jauhar, S. K., Cucerzan, S., and Hwang, S. J. Researchagent: Iterative research idea generation over scientific literature with large language models. In *Proceedings of the 2025 Conference of the Nations of the Americas Chapter of the Association for Computational Linguistics: Human Language Technologies (Volume 1: Long Papers)*, pp. 6709–6738, 2025.

Black, K., Brown, N., Driess, D., Esmail, A., Equi, M., Finn, C., Fusai, N., Groom, L., Hausman, K., Ichter, B., et al.  $\pi_0$ : A vision-language-action flow model for general robot control. *arXiv preprint arXiv:2410.24164*, 2024.

Brohan, A., Chebotar, Y., Finn, C., Hausman, K., Herzog, A., Ho, D., Ibarz, J., Irpan, A., Jang, E., Julian, R., et al. Do as i can, not as i say: Grounding language in robotic affordances. In *Conference on robot learning*, pp. 287–318. PMLR, 2023.

Chen, W., Su, Y., Zuo, J., Yang, C., Yuan, C., Chan, C.-M., Yu, H., Lu, Y., Hung, Y.-H., Qian, C., et al. Agentverse: Facilitating multi-agent collaboration and exploring emergent behaviors. In *ICLR*, 2024.

Cohen, M. W., Aga, M., and Weinberg, T. Genetic algorithm software system for analog circuit design. *Procedia CIRP*, 36:17–22, 2015.

Eriksson, D., Pearce, M., Gardner, J., Turner, R. D., and Poloczek, M. Scalable global optimization via local bayesian optimization. *Advances in neural information processing systems*, 32, 2019.

Guo, S., Deng, C., Wen, Y., Chen, H., Chang, Y., and Wang, J. DS-agent: Automated data science by empowering large language models with case-based reasoning. In *Proceedings of the 41st International Conference on Machine Learning*, volume 235 of *Proceedings of Machine Learning Research*, pp. 16813–16848. PMLR, 2024.

Hong, S., Lin, Y., Liu, B., Liu, B., Wu, B., Zhang, C., Li, D., Chen, J., Zhang, J., Wang, J., et al. Data interpreter: An llm agent for data science. In *Findings of the Association for Computational Linguistics: ACL 2025*, pp. 19796–19821, 2025.

Jimenez, C. E., Yang, J., Wettig, A., Yao, S., Pei, K., Press, O., and Narasimhan, K. Swe-bench: Can language models resolve real-world github issues? *arXiv preprint arXiv:2310.06770*, 2023.

Kochar, D. V., Wang, H., Chandrakasan, A. P., and Zhang, X. Ledro: Llm-enhanced design space reduction and optimization for analog circuits. In *2025 IEEE International Conference on LLM-Aided Design (ICLAD)*, pp. 141–148. IEEE, 2025.

Lai, Y., Poddar, S., Lee, S., Chen, G., Hu, M., Yu, B., Luo, P., and Pan, D. Z. Analogcoder-pro: Unifying analog circuit generation and optimization via multi-modal llms. *arXiv preprint arXiv:2508.02518*, 2025.

Liu, B., Zhao, D., Reynaert, P., and Gielen, G. G. Gaspad: A general and efficient mm-wave integrated circuit synthesis method based on surrogate model assisted evolutionary algorithm. *IEEE Transactions on Computer-Aided Design of Integrated Circuits and Systems*, 33(2): 169–182, 2014.

Liu, C. and Chitnis, D. Eeschematic: Multimodal-llm based ai agent for schematic generation of analog circuit. *arXiv preprint arXiv:2510.17002*, 2025a.

Liu, C. and Chitnis, D. Eesizer: Llm-based ai agent for sizing of analog and mixed signal circuit. *arXiv preprint arXiv:2509.25510*, 2025b.

Liu, C., Chen, W., Peng, A., Du, Y., Du, L., and Yang, J. Am-pagent: An llm-based multi-agent system for multi-stage amplifier schematic design from literature for process and performance porting. *arXiv preprint arXiv:2409.14739*, 2024.

Lyu, W., Yang, F., Yan, C., Zhou, D., and Zeng, X. Batch bayesian optimization via multi-objective acquisition ensemble for automated analog circuit design. In *International conference on machine learning*, pp. 3306–3314. PMLR, 2018.

Pessoa, T., Lourenço, N., Martins, R., Póvoa, R., and Horta, N. Enhanced analog and rf ic sizing methodology using pca and nsga-ii optimization kernel. In *2018 Design, Automation & Test in Europe Conference & Exhibition (DATE)*, pp. 660–665. IEEE, 2018.

Ren, X., Zang, Q., and Guo, Z. Simugen: Multi-modal agentic framework for constructing block diagram-based simulation models. *arXiv preprint arXiv:2506.15695*, 2025.

Settaluri, K., Haj-Ali, A., Huang, Q., Hakhamaneshi, K., and Nikolic, B. Autockt: Deep reinforcement learning of analog circuit designs. *arXiv preprint arXiv:2001.01808*, 2020.

Shahriari, B., Swersky, K., Wang, Z., Adams, R. P., and De Freitas, N. Taking the human out of the loop: A review of bayesian optimization. *Proceedings of the IEEE*, 104 (1):148–175, 2015.

Somayaji, N. K. and Li, P. Llm-uso: Large language model-based universal sizing optimizer. *IEEE Transactions on Computer-Aided Design of Integrated Circuits and Systems*, 2025.

Taherzadeh-Sani, M., Lotfi, R., Zare-Hoseini, H., and Shoaei, O. Design optimization of analog integrated circuits using simulation-based genetic algorithm. In *Signals, Circuits and Systems, 2003. SCS 2003. International Symposium on*, volume 1, pp. 73–76. IEEE, 2003.

Touloupas, K., Chouridis, N., and Sotiriadis, P. P. Local bayesian optimization for analog circuit sizing. In *2021 58th ACM/IEEE design automation conference (DAC)*, pp. 1237–1242. IEEE, 2021.

Vogt, H., Atkinson, G., Nenzi, P., and Warning, D. Ngspice user’s manual version 34 (ngspice release version), 2021.

Wang, H., Yang, J., Lee, H.-S., and Han, S. Learning to design circuits. *arXiv preprint arXiv:1812.02734*, 2018.

Wang, H., Wang, K., Yang, J., Shen, L., Sun, N., Lee, H.-S., and Han, S. Gcn-rl circuit designer: Transferable transistor sizing with graph neural networks and reinforcement learning. In *2020 57th ACM/IEEE Design Automation Conference (DAC)*, pp. 1–6. IEEE, 2020.

Wang, X., Li, B., Song, Y., Xu, F. F., Tang, X., Zhuge, M., Pan, J., Song, Y., Li, B., Singh, J., et al. Opendevin: An open platform for ai software developers as generalist agents. *arXiv preprint arXiv:2407.16741*, 3, 2024.

Wolfe, G. and Vemuri, R. Extraction and use of neural network models in automated synthesis of operational amplifiers. *IEEE Transactions on Computer-Aided Design of Integrated Circuits and Systems*, 22(2):198–212, 2003.

Xu, S., Zhi, H., Li, J., and Shan, W. Llmacd: An llm-based analog circuit designer driven by behavior parameters. In *2025 International Symposium of Electronics Design Automation (ISED)*, pp. 157–162. IEEE, 2025.

Yamada, Y., Lange, R. T., Lu, C., Hu, S., Lu, C., Foerster, J., Clune, J., and Ha, D. The ai scientist-v2: Workshop-level automated scientific discovery via agentic tree search. *arXiv preprint arXiv:2504.08066*, 2025.

Yang, K.-E., Tsai, C.-Y., Shen, H.-H., Chiang, C.-F., Tsai, F.-M., Wang, C.-A., Ting, Y., Yeh, C.-S., and Lai, C.-T. Trust-region method with deep reinforcement learning in analog design space exploration. In *2021 58th ACM/IEEE design automation conference (DAC)*, pp. 1225–1230. IEEE, 2021.

Yao, S., Zhao, J., Yu, D., Du, N., Shafran, I., Narasimhan, K. R., and Cao, Y. React: Synergizing reasoning and acting in language models. In *The eleventh international conference on learning representations*, 2022.

Yin, Y., Wang, Y., Xu, B., and Li, P. Ado-llm: Analog design bayesian optimization with in-context learning of large language models. In *Proceedings of the 43rd IEEE/ACM International Conference on Computer-Aided Design*, pp. 1–9, 2024.

Zhang, J., Bao, J., Huang, Z., Zeng, X., and Lu, Y. Automated design of complex analog circuits with multiagent based reinforcement learning. In *2023 60th ACM/IEEE Design Automation Conference (DAC)*, pp. 1–6. IEEE, 2023.

## A. Details of AMS-SIZINGBENCH

### A.1. AMS-SIZINGBENCH Benchmark Circuit Summary

Table 4. AMS-SIZINGBENCH Benchmark Circuit Summary

Circuit	Type	Diff.	#T	Description	Circuit	Type	Diff.	#T	Description
inverter	Logic	Easy	2	Basic CMOS logic gate that inverts the input signal.	five_trans_ota	Amp	Med.	6	Compact operational transconductance amplifier with minimal transistor count.
buffer	Logic	Easy	4	Cascaded inverter structure for restoring logic levels.	vco	Osc.	Med.	10	Voltage-controlled oscillator with frequency tunable by control voltage.
nand_gate	Logic	Easy	4	CMOS logic gate implementing the NAND Boolean function.	telescopic_ota	Amp	Med.	10	High-gain telescopic cascode OTA using stacked devices.
resistive_load_amp	Amp	Easy	1	Single-transistor amplifier using a resistive load.	current_mirror_ota	Amp	Med.	10	OTA based on current-mirror biasing for gain and matching.
diode_load_amp	Amp	Easy	2	Amplifier employing a diode-connected load.	folded_cascode_ota	Amp	Med.	10	Folded cascode OTA enabling wide input common-mode range.
ring_oscillator (3-stage)	Osc.	Med.	6	Three-stage inverter loop generating oscillation.	ldo	Power	Hard	11	Low-dropout voltage regulator operating under limited headroom.
bandgap	Ref.	Hard	12	Temperature-stable voltage reference circuit.	folded_cascode_ota_low_pass_filter	Filter	Hard	10	Low-pass active filter implemented using a Sallen-Key topology with a folded-cascode OTA.
switched_capacitor	SC	Hard	10	Switched-capacitor circuit with sampling network and OTA.	folded_cascode_ota_high_pass_filter	Filter	Hard	10	High-pass active filter implemented using a Sallen-Key topology with a folded-cascode OTA.
xor_gate	Logic	Hard	14	CMOS logic gate implementing the XOR operation.	folded_cascode_ota_band_pass_filter	Filter	Hard	10	Band-pass OTA-based active filter implemented using a Sallen-Key topology with a folded-cascode OTA.
AZC	Amp	Hard	25	Active-Zero Compensation technique for offset and low-frequency error reduction.	fdgb	Amp	Hard	26	Fully Differential Gain-Boosting Amplifier architecture.
nmcnr	Amp	Hard	24	Nested Miller Compensation with Nulling Resistor for stability enhancement.	smc	Amp	Hard	24	Simple Miller Compensation three-stage amplifier.
dfcfc	Amp	Hard	26	Damping Factor Control Frequency Compensation for multi-stage amplifiers.	iac	Amp	Hard	35	Indirect Amplifier Compensation technique for high-speed stability.

### A.2. AMS-SIZINGBENCH Example

```

pdk_lib_path: "..../skywater-pdk-libs-sky130_fd_pr/combined_models/sky130.lib.spice"
align_pdk_path: "..../ALIGN-pdk-sky130/SKY130_PDK/"
pex_script_path: "..../ALIGN-public/test_magic_pex.py"
results_dir: "./telescopic_ota_test_folder"

user_specs: "Primary goal: Maximize DC gain and UGBW while minimizing power consumption for a telescopic OTA with 1pF load."
user_specs_metric: "fom > 0.100 AND dc_gain_db > 55 AND ugbw > 10 AND power_dc < 50"

params:
    L: 0.15
    vdd: 1.8
    vcm: 0.7
    cload: 1e-12
    ibias: 10e-6
    vbiasp1: 1.15

variable:
    W_tail_base: null
    W_diff_base: null
    W_casc_base: null
    W_load_base: null

W_values: [0.84, 1.05, 1.26, 1.47, 1.68, 1.89, 2.10, 2.31, 2.52]

```

```

width_scales:
  W_tail: [W_tail_base, 2]
  W_diff: [W_diff_base, 4]
  W_casc: [W_casc_base, 2]
  W_load: [W_load_base, 2]

subckt_name: TELESCOPIC_OTA
subckt_pins:
  - VBIASN
  - VBIASNC
  - VBIASP1
  - VBIASP2
  - VINN
  - VINP
  - VOUTN
  - VOUTP
  - VDD
  - "0"

testbench_signals:
  VBIASN: VBIASN
  VBIASNC: VBIASNC
  VBIASP1: VBIASP1
  VBIASP2: VBIASP2
  VINN: VINN
  VINP: VINP
  VOUTN: VOUTN
  VOUTP: VOUTP
  VDD: VDD
  "0": "0"

metrics:
  - dc_gain_db
  - ugbw
  - power_dc
  - fom

base_metrics:
  gain_db:
    name: "Gain"
    unit: "dB"
    format: ".1f"
    degradation_key: "gain_percent"

  power_uw:
    name: "Power"
    unit: "μW"
    format: ".1f"
    degradation_key: "power_percent"

  ugbw_mhz:
    name: "UGBW"
    unit: "MHz"
    format: ".1f"
    degradation_key: "ugbw_percent"

fom:
  name: "FOM"
  unit: ""
  format: ".3f"
  degradation_key: "fom_percent"

ota_subckt_template: |
  .subckt TELESCOPIC_OTA VBIASN VBIASNC VBIASP1 VBIASP2 VINN VINP VOUTN VOUTP VDD 0
  * Tail current sources

```

```

xm1 ID VBIASN 0 0 sky130_fd_pr_nfet_01v8 w={W_tail} l={L}
xm2 NET10 VBIASN 0 0 sky130_fd_pr_nfet_01v8 w={W_tail} l={L}
* Differential pair
xm3 NET8 VINP NET10 0 sky130_fd_pr_nfet_01v8 w={W_diff} l={L}
xm4 NET014 VINN NET10 0 sky130_fd_pr_nfet_01v8 w={W_diff} l={L}
* NMOS cascode (use VBIASNC here)
xm5 VOUTN VBIASNC NET8 0 sky130_fd_pr_nfet_01v8 w={W_casc} l={L}
xm6 VOUTP VBIASNC NET014 0 sky130_fd_pr_nfet_01v8 w={W_casc} l={L}
* PMOS cascode
xm7 VOUTN VBIASPC1 NET06 VDD sky130_fd_pr_pfet_01v8 w={W_casc} l={L}
xm8 VOUTP VBIASPC1 NET012 VDD sky130_fd_pr_pfet_01v8 w={W_casc} l={L}
* PMOS current source
xm9 NET06 VBIASPC2 VDD VDD sky130_fd_pr_pfet_01v8 w={W_load} l={L}
xm10 NET012 VBIASPC2 VDD VDD sky130_fd_pr_pfet_01v8 w={W_load} l={L}
.ends TELESCOPIC_OTA

testbench_template: |
* Telescopic OTA Simulation
.lib {pdk_lib_path} tt
{ota_subckt}
* Power supply
VDD VDD 0 DC {vdd}
* Bias Generation
IBIAS_N VDD VBIASN DC {ibias}
XMN_BIAS VBIASN VBIASN 0 0 sky130_fd_pr_nfet_01v8 w={W_tail} l={L}
IBIAS_P VBIASPC2 0 DC {ibias}
XMP_BIAS VBIASPC2 VBIASPC2 VDD VDD sky130_fd_pr_pfet_01v8 w={W_load} l={L}
VBIASPC1 VBIASPC1 0 DC={vbiaspc1}
IBIAS_NC VDD VBIASNC DC {ibias}
XMN_BIASNC VBIASNC VBIASNC 0 0 sky130_fd_pr_nfet_01v8 w={W_casc} l={L}
* Differential inputs
VINP VINP 0 DC {vcm} AC 0.5
VINN VINN 0 DC {vcm} AC -0.5
* OTA instance
XOTA {inst_pins} {subckt_name}
* Load capacitors
CLOADP VOUTP 0 {cload}
CLOADN VOUTN 0 {cload}

.op
.control
.op
* Power
let vdd_current = abs(i(VDD))
let power_dc = vdd_current * {vdd}
echo "==== POWER ==="
print vdd_current power_dc
* AC analysis
ac dec 100 1 10g

let vout_diff = v(VOUTP) - v(VOUTN)
let gain_db = db(vout_diff)
let dc_gain_db = gain_db[0]

echo "==== DC GAIN ==="
print dc_gain_db

* UGBW
if dc_gain_db > 0
  meas ac ugbw WHEN gain_db=0 CROSS=1
end
quit
.endc
.end

```

### A.3. Sizing Variables and Specification

This section provides the details of each circuit in the AMS-SIZINGBENCH input and output specifications, and the simulation checklist used to validate each circuit block against design requirements.

Table 5. Circuit blocks: inputs, output specifications, and simulation checklist.

Circuit name	Input signal(s)	Output specification(s)	Simulation part (what to run)
Inverter	$V_{DD} = 1.8\text{ V}$ ; $V_{IN}$ DC sweep from 0 to 1.8 V with 10 mV step and rail-to-rail pulse with 100 ps rise/fall time; load capacitance $C_L = 10\text{ fF}$	Maximum DC voltage gain (dB); average propagation delay at 50% threshold ( $t_{PLH}$ , $t_{PHL}$ ); dynamic power consumption.	DC sweep for transfer characteristic and gain extraction; transient analysis for delay and power; static and dynamic power separation using supply current; transistor width sweep for performance optimization
Buffer	$V_{DD} = 1.8\text{ V}$ ; $V_{IN}$ rail-to-rail pulse from 0 to 1.8 V with 100 ps rise/fall time and 4 ns period; DC sweep from 0 to 1.8 V with 10 mV step; load capacitance $C_L = 10\text{ fF}$	Maximum DC voltage gain (dB); average propagation delay at 50% threshold ( $t_{PLH}$ , $t_{PHL}$ ); dynamic power consumption.	DC sweep for overall buffer gain extraction; transient analysis for propagation delay and switching behavior; average and static power estimation from supply current; dynamic power computed as average minus static power; transistor width sweep across both stages for performance optimization
NAND (2-input)	$V_{DD} = 1.8\text{ V}$ ; two digital inputs $A$ and $B$ driven by piecewise-linear waveforms to exercise NAND switching cases, including $B$ rising and falling while $A$ is held high; rise/fall time 100 ps; operating frequency 100 MHz; load capacitance $C_L = 10\text{ fF}$	Propagation delays $t_{PHL}$ and $t_{PLH}$ measured at 50% $V_{DD}$ threshold; average propagation delay; static, dynamic, and total power consumption; energy per transition; output voltage levels $V_{OH}$ and $V_{OL}$ ; noise margins (NMH, NML)	Operating-point analysis for static current and static power; transient simulation for delay, dynamic power, and energy-per-transition extraction; delay measured from input $B$ to output $Y$ at 50% $V_{DD}$ crossings; output voltage extrema used to compute $V_{OH}$ , $V_{OL}$ , and noise margins;
Resistive-Load Amplifier (Common-Source + $R_L$ )	$V_{DD} = 1.8\text{ V}$ ; input $V_{IN}$ biased at $V_{bias} = 0.6\text{ V}$ with small-signal excitation $v_{ac} = 1\text{ mV}$ ; load $R_L = 50\text{ k}\Omega$ and $C_L = 10\text{ fF}$ ; AC sweep from 1 Hz to 10 GHz	Small-signal voltage gain (dB); $-3\text{ dB}$ bandwidth (MHz); DC power consumption ( $\mu\text{W}$ ); and output voltage swing (V)	Operating-point analysis to extract $I_{DD}$ and $V_{OUT,DC}$ ; AC analysis (decade sweep) to obtain gain response and determine $-3\text{ dB}$ bandwidth; power computed from $I_{DD}V_{DD}$ ; output swing estimated from the DC bias point.
Diode-Load Amplifier (Common-Source + Diode-Connected Load)	$V_{DD} = 1.8\text{ V}$ ; input $V_{IN}$ biased at 0.6 V with small-signal AC excitation of 1 mV; load capacitance $C_L = 10\text{ fF}$ ; AC frequency sweep from 1 Hz to 10 GHz	Small-signal voltage gain (dB); $-3\text{ dB}$ bandwidth (MHz); DC power consumption ( $\mu\text{W}$ ); output voltage swing (V)	Operating-point analysis to extract supply current and DC output voltage; AC analysis to obtain gain response and determine $-3\text{ dB}$ bandwidth; power computed from $I_{DD}V_{DD}$ ; output swing estimated from the DC operating point; parametric sweep of input and load transistor dimensions
3-stage ring oscillator	$V_{DD} = 1.8\text{ V}$ ; three cascaded CMOS inverters connected in a ring; initial condition applied to one node for startup; load capacitance $C_L = 10\text{ fF}$ ; transient simulation	Oscillation frequency (MHz); oscillation period (ns); average power consumption ( $\mu\text{W}$ ); delay per inverter stage (ps)	Transient simulation to capture steady-state oscillation; period measured from consecutive rising zero-crossings at 50% $V_{DD}$ ; oscillation frequency computed from period; average power calculated from mean supply current; delay per stage extracted as period/(2N) for $N = 3$ stages
Bandgap reference	Supply voltage $V_{DD}$ with nominal value 2.0 V; DC supply sweep from 1.8 V to 3.3 V for line regulation measurement; AC small-signal excitation at the supply for PSRR analysis; temperature set to 27°C	Reference voltage $V_{REF}$ (V); DC power consumption ( $\mu\text{W}$ ); line regulation (%/V); power supply rejection ratio (PSRR, dB)	Operating-point analysis to extract $V_{REF}$ and supply current; DC sweep of $V_{DD}$ to evaluate line regulation; AC analysis with supply perturbation to extract PSRR; power computed from supply current and nominal $V_{DD}$
Current-Mirror OTA	$V_{DD} = 1.8\text{ V}$ ; tail bias current $I_{BIAS} = 20\text{ }\mu\text{A}$ ; differential input with common-mode voltage $V_{CM} = 0.9\text{ V}$ and small-signal excitation (+0.5 / -0.5 AC); load capacitance $C_L = 1\text{ pF}$	DC voltage gain (dB); unity-gain bandwidth (UGBW, MHz); DC power consumption ( $\mu\text{W}$ )	Operating-point analysis to extract supply current and DC power; AC analysis to obtain differential gain response; DC gain extracted at low frequency; unity-gain bandwidth measured at 0 dB gain crossing;
Five-transistor OTA	$V_{DD} = 1.8\text{ V}$ ; tail bias current $I_{BIAS} = 20\text{ }\mu\text{A}$ ; differential input with common-mode voltage $V_{CM} = 0.9\text{ V}$ and small-signal excitation (+0.5 / -0.5 AC); load capacitance $C_L = 1\text{ pF}$	DC voltage gain (dB); unity-gain bandwidth (UGBW, MHz); DC power consumption ( $\mu\text{W}$ )	Operating-point analysis to extract supply current and DC power; AC analysis to obtain differential gain response; DC gain extracted at low frequency; unity-gain bandwidth measured at 0 dB gain crossing;

Circuit name	Input signal(s)	Output specification(s)	Simulation part (what to run)
Telescopic cascode OTA	$V_{DD} = 1.8\text{ V}$ ; tail bias current $I_{BIAS} = 10\text{ }\mu\text{A}$ ; differential input with common-mode voltage $V_{CM} = 0.7\text{ V}$ and small-signal excitation ( $+0.5 / -0.5\text{ AC}$ ); bias voltages $V_{BIASN}$ , $V_{BIASNC}$ , $V_{BIASPI} = 1.15\text{ V}$ , and $V_{BIASP2}$ ; differential load capacitance $C_L = 1\text{ pF}$ per output	DC differential voltage gain (dB); unity-gain bandwidth (UGBW, MHz); DC power consumption ( $\mu\text{W}$ )	Operating-point analysis to establish bias currents and extract DC power; AC analysis of differential output to obtain gain response; DC gain extracted at low frequency; unity-gain bandwidth measured at 0 dB differential gain crossing; parametric sweep of tail, input, cascode, and load device widths to evaluate gain-bandwidth-power trade-offs
Switched-Capacitor Circuit	$V_{DD} = 1.8\text{ V}$ ; differential OTA biased with $I_{BIAS} = 10\text{ }\mu\text{A}$ ; input signal $V_{IN}$ with DC bias around mid-supply and AC amplitude 0.25 V; two non-overlapping clock phases at 1 MHz; sampling, holding, and load capacitors ( $C_{samp}$ , $C_{hold}$ , $C_{load}$ )	Closed-loop gain (dB) and gain error; settling time (ns); charge injection (mV); DC power consumption ( $\mu\text{W}$ ); total harmonic distortion (THD, dB); output voltage swing (V); unity-gain bandwidth (UGBW, MHz); DC gain (dB); phase margin (deg)	Transient simulation of a switched-capacitor integrator using two non-overlapping clock phases at 1 MHz; operating-point analysis to obtain DC bias and initial output swing; closed-loop gain extracted from steady-state output voltage after multiple clock cycles; settling time measured using a 1% error criterion relative to final value; charge injection quantified from voltage disturbance at the sampling node during clock transitions; average supply current used to compute DC power consumption; FFT-based spectral analysis of the output waveform to extract total harmonic distortion (THD); separate open-loop OTA AC analysis performed to extract DC gain, unity-gain bandwidth (UGBW), and phase margin
Low-Dropout Regulator (LDO)	Supply voltage $V_{DD} = 1.8\text{ V}$ with DC sweep from $0.9V_{DD}$ to $1.1V_{DD}$ ; reference voltage $V_{REF} = 0.6\text{ V}$ ; programmable load current swept from $0.1I_{LOAD}$ to $2I_{LOAD}$ (up to 20 mA); bias current $I_{BIAS} = 10\text{ }\mu\text{A}$	Regulated output voltage $V_{OUT}$ (V); dropout voltage (mV); line regulation (mV/V); load regulation (mV/mA); power supply rejection ratio (PSRR, dB); DC power consumption ( $\mu\text{W}$ ); output voltage variation over temperature (V)	Operating-point analysis to establish nominal bias and output voltage; DC supply-voltage sweep from $0.9V_{DD}$ to $1.1V_{DD}$ to extract dropout voltage and line regulation; DC load-current sweep from $0.1I_{LOAD}$ to $2I_{LOAD}$ to evaluate load regulation; AC analysis with small-signal supply injection to extract PSRR; DC power consumption computed from measured supply and load currents
Voltage-Controlled Oscillator	Supply voltage $V_{DD} = 1.8\text{ V}$ ; control voltage $V_{CTRL}$ swept from 0 to 1.8 V; five-stage CMOS ring oscillator with inverter-based delay cells; temperature set to $27^\circ\text{C}$	Oscillation frequency (Hz); DC power consumption ( $\mu\text{W}$ ); tuning range (%); frequency at minimum and maximum control voltage; VCO gain (MHz/V)	Transient simulation of a five-stage CMOS ring oscillator with voltage-dependent load capacitance to induce frequency tuning; a single control-voltage run used to extract steady-state oscillation frequency and DC power consumption from time-domain waveforms; oscillation frequency measured from rising zero-crossings after steady-state is reached; power computed from the median supply current during steady-state operation; extended characterization performed by sweeping the control voltage across the specified range and repeating transient simulations at each point to extract frequency tuning behavior; tuning range computed from minimum and maximum oscillation frequencies; average VCO gain (MHz/V) extracted from local frequency-voltage slopes; statistical filtering applied to remove high-power outliers before aggregating power metrics; overall performance summarized using a composite figure of merit (FOM)
XOR Gate (2-Input CMOS XOR with Transmission Gates)	$V_{DD} = 1.8\text{ V}$ ; two digital inputs $A$ and $B$ driven by piecewise-linear waveforms to exercise XOR switching conditions, including rising and falling transitions of $B$ while $A$ is held high; rise/fall time 100 ps; operating frequency 100 MHz; load capacitance $C_L = 10\text{ fF}$	Propagation delays $t_{PHL}$ and $t_{PLH}$ (ps); average propagation delay (ps); static, dynamic, and total power consumption ( $\mu\text{W}$ ); energy per transition (fJ); output voltage levels $V_{OH}$ and $V_{OL}$ (V); noise margins (NMH, NML)	Operating-point analysis to extract static supply current and static power; transient simulation with representative input transitions to measure propagation delays at the 50% $V_{DD}$ threshold; average dynamic power computed from mean supply current during switching activity; energy per transition calculated from dynamic power and switching frequency; output voltage extrema used to extract $V_{OH}$ , $V_{OL}$ , and noise margins
Active Zero Compensated OTA (AZC)	$V_{DD} = 1.8\text{ V}$ ; differential input with $V_{CM} = 0.3\text{ V}$ ; small-signal AC excitation ( $+0.5 / -0.5$ ); bias current $I_{BIAS} = 1\text{ }\mu\text{A}$ ; load $R_L = 25\text{ k}\Omega$ , $C_L = 15\text{ nF}$	DC voltage gain (dB); unity-gain bandwidth (UGBW); DC power consumption ( $\mu\text{W}$ )	Operating-point analysis to extract supply current and DC power; AC analysis (1 Hz–10 GHz) with differential excitation to obtain gain response; DC gain extracted from low-frequency AC magnitude; unity-gain bandwidth measured at 0 dB gain crossing;
Damping-Factor-Controlled Folded-Cascode OTA (DFCFC)	$V_{DD} = 1.8\text{ V}$ ; differential input with $V_{CM} = 0.9\text{ V}$ ; small-signal AC excitation ( $+0.5 / -0.5$ ); bias current $I_{BIAS} = 10\text{ }\mu\text{A}$ ; load $R_L = 25\text{ k}\Omega$ , $C_L = 15\text{ nF}$	DC voltage gain (dB); unity-gain bandwidth (UGBW); DC power consumption ( $\mu\text{W}$ )	Operating-point analysis to establish bias currents and compute DC power from supply current; AC analysis (1 Hz–10 GHz) with differential excitation to obtain gain response; DC gain extracted from low-frequency AC magnitude; unity-gain bandwidth measured at 0 dB gain crossing;

Circuit name	Input signal(s)	Output specification(s)	Simulation part (what to run)	
Fully Differential Gain-Boosted OTA (FDGB)	$V_{DD} = 1.8\text{ V}$ ; fully differential input with $V_{CM} = 0.9\text{ V}$ ; small-signal AC excitation ( $+0.5/-0.5$ ); bias current $I_{BIAS} = 10\text{ }\mu\text{A}$ ; differential load $R_L = 25\text{ k}\Omega$ , $C_L = 15\text{ nF}$ per output	DC differential voltage gain (dB); unity-gain bandwidth (UGBW); DC power consumption ( $\mu\text{W}$ ).	Operating-point analysis to establish bias currents and compute DC power from supply current; AC analysis (1 Hz–10 GHz) with fully differential excitation and differential output sensing ( $V_{OUTP} - V_{OUTN}$ ); DC gain extracted from low-frequency differential AC magnitude; unity-gain bandwidth measured at 0 dB differential gain crossing.	
Indirectly Compensated OTA (IAC)	$V_{DD} = 1.8\text{ V}$ ; differential input with $V_{CM} = 0.9\text{ V}$ ; small-signal AC excitation ( $+0.5/-0.5$ ); bias current $I_{BIAS} = 47\text{ }\mu\text{A}$ ; load $R_L = 25\text{ k}\Omega$ , $C_L = 15\text{ nF}$	DC voltage gain (dB); unity-gain bandwidth (UGBW); DC power consumption ( $\mu\text{W}$ ).	Operating-point analysis to establish bias currents and compute DC power from supply current; AC analysis (1 Hz–10 GHz) with differential excitation to obtain gain response; DC gain extracted from low-frequency AC magnitude; unity-gain bandwidth measured at 0 dB gain crossing; compensation behavior governed by indirect Miller network.	
Nested-Miller OTA with Nulling Resistor (NM-CNR)	$V_{DD} = 1.8\text{ V}$ ; differential input with $V_{CM} = 0.9\text{ V}$ ; small-signal AC excitation ( $+0.5/-0.5$ ); bias current $I_{BIAS} = 19\text{ }\mu\text{A}$ ; load $R_L = 25\text{ k}\Omega$ , $C_L = 15\text{ nF}$	DC voltage gain (dB); unity-gain bandwidth (UGBW); DC power consumption ( $\mu\text{W}$ ).	Operating-point analysis to establish bias currents and compute DC power from supply current; AC analysis (1 Hz–10 GHz) with differential excitation to obtain gain response; DC gain extracted from low-frequency AC magnitude; unity-gain bandwidth measured at 0 dB gain crossing; nested Miller compensation with nulling resistor used for pole-zero placement.	
Single-Miller-Compensated (SMC)	OTA	$V_{DD} = 1.8\text{ V}$ ; differential input with $V_{CM} = 0.9\text{ V}$ ; small-signal AC excitation ( $+0.5/-0.5$ ); bias current $I_{BIAS} = 20\text{ }\mu\text{A}$ ; load $R_L = 25\text{ k}\Omega$ , $C_L = 15\text{ nF}$	DC voltage gain (dB); unity-gain bandwidth (UGBW); DC power consumption ( $\mu\text{W}$ ).	Operating-point analysis to establish bias currents and compute DC power from supply current; AC analysis (1 Hz–10 GHz) with differential excitation to obtain gain response; DC gain extracted from low-frequency AC magnitude; unity-gain bandwidth measured at 0 dB gain crossing; dominant-pole stabilization achieved via single Miller compensation capacitor; FOM computed from extracted gain, UGBW, and power.
Folded-cascode OTA		$V_{DD} = 1.8\text{ V}$ ; tail current $I_{TAIL} = 10\text{ }\mu\text{A}$ ; differential input with common-mode voltage $V_{CM} = 0.9\text{ V}$ and small-signal excitation ( $+0.5/-0.5$ AC); bias voltages $V_{BN} = 0.7\text{ V}$ and $V_{BP} = 1.0\text{ V}$ ; load capacitance $C_L = 1\text{ pF}$	DC voltage gain (dB); unity-gain bandwidth (UGBW, MHz); DC power consumption ( $\mu\text{W}$ ).	Operating-point analysis to establish bias currents and extract DC power; AC analysis to obtain differential gain response; DC gain measured as maximum low-frequency gain; unity-gain bandwidth extracted at 0 dB gain crossing; parametric sweep of device widths to optimize gain-bandwidth-power trade-offs under a fixed 1 pF load.
Folded-Cascode OTA with Integrated Low-Pass Filter (LPF)		$V_{DD} = 1.8\text{ V}$ ; differential input with $V_{CM} = 0.9\text{ V}$ ; small-signal AC excitation ( $+0.5/-0.5$ ); tail current $I_{TAIL} = 10\text{ }\mu\text{A}$ ; bias voltages $V_{BN} = 0.6\text{ V}$ , $V_{BP} = 0.6\text{ V}$ ; load capacitance $C_L = 1\text{ pF}$	Low-pass cutoff frequency ( $f_c$ ); passband gain (dB); roll-off rate (dB/dec); stopband attenuation (dB); quality factor ( $Q$ ); DC power consumption ( $\mu\text{W}$ ).	Operating-point analysis to establish bias currents and DC operating conditions; AC analysis (1 Hz–10 GHz) with differential excitation to extract frequency response; cutoff frequency determined from $-3\text{ dB}$ point; passband gain measured at low frequency; roll-off and stopband attenuation extracted from AC magnitude slope; quality factor computed from filter parameters; power calculated from supply current.
Folded-Cascode OTA with Integrated High-Pass Filter (HPF)		$V_{DD} = 1.8\text{ V}$ ; differential input with $V_{CM} = 0.9\text{ V}$ ; small-signal AC excitation ( $+0.5/-0.5$ ); tail current $I_{TAIL} = 10\text{ }\mu\text{A}$ ; bias voltages $V_{BN} = 0.7\text{ V}$ , $V_{BP} = 1.0\text{ V}$ ; load capacitance $C_L = 1\text{ pF}$	High-pass cutoff frequency ( $f_c$ ); passband gain (dB); roll-off rate (dB/dec); stopband attenuation (dB); quality factor ( $Q$ ); DC power consumption ( $\mu\text{W}$ ).	Operating-point analysis to establish bias currents and DC operating conditions; AC analysis (1 Hz–10 GHz) with differential excitation to extract frequency response; cutoff frequency determined from $-3\text{ dB}$ point; passband gain measured at high frequency; roll-off and stopband attenuation extracted from AC magnitude slope; quality factor computed from filter parameters; power calculated from supply current.
Folded-Cascode OTA with Integrated Band-Pass Filter (BPF)	OTA	$V_{DD} = 1.8\text{ V}$ ; differential input with $V_{CM} = 0.9\text{ V}$ ; small-signal AC excitation ( $+0.5/-0.5$ ); tail current $I_{TAIL} = 10\text{ }\mu\text{A}$ ; bias voltages $V_{BN} = 0.7\text{ V}$ , $V_{BP} = 1.0\text{ V}$ ; load capacitance $C_L = 1\text{ pF}$	Center frequency ( $f_0$ ); bandwidth (Hz); peak gain (dB); quality factor ( $Q$ ); DC power consumption ( $\mu\text{W}$ ).	Operating-point analysis to establish bias currents and DC operating conditions; AC analysis (1 Hz–10 GHz) with differential excitation to extract band-pass frequency response; center frequency identified at peak gain; bandwidth measured between $-3\text{ dB}$ points; quality factor computed as $Q = f_0/\text{BW}$ ; peak gain extracted from AC magnitude response; power calculated from supply current;

## B. Prompts used of AUTOSizer

### B.1. Circuit Understanding Prompt

#### Circuit Understanding Prompt

You are an expert analog circuit designer. Your task is to understand the circuit topology and the role of each component, with focus on the optimization variables.

```
**Circuit Name:** {subckt_name}
**Circuit Netlist:** 
```
{ota_subckt_template}
```

**Fixed Design Parameters (DO NOT optimize):**
{params}

**Optimization Variables (WILL be optimized):**
{variables}

**Testbench:** 
```
{testbench_template}
```

**Performance Metrics:** 
The following metrics will be evaluated:
{metrics_list}

## Your Task - Part 1: Circuit Analysis

**IMPORTANT:** Keep each main section to 3-5 sentences total. Focus on how the OPTIMIZATION VARIABLES affect circuit performance, not the fixed parameters.**

### 1. Circuit Topology Overview (3-5 sentences total)
Identify the circuit type from the netlist, describe the overall architecture, and explain the signal flow from input to output.

### 2. Optimization Variables Mapping (3-5 sentences total)
For each optimization variable, identify which transistors it controls (from the netlist and scaling rules). Group the variables by the functional role of transistors they control.

### 3. Optimization Variables Impact on Performance (3-5 sentences total for each sub-section)
Impact on {metric_name}:
Explain how the optimization variables {{variables}} affect {metric_key}.
Focus on which variables have the strongest impact on {metric_key} and why.

### 4. Variable Interactions (3-5 sentences total)
Describe any interactions between optimization variables: which must be scaled together for matching, which have conflicting effects, and which have synergistic effects.

### 5. Key Insights for Optimization (3-5 bullet points, 1 sentence each)
Provide 3-5 critical insights about optimizing this circuit, focusing on the optimization variables.

## Output Requirements

You must provide your analysis in **valid JSON format only**.
```

Your response should contain ONLY the JSON object with no additional text before or after.

```

### JSON Structure
```
{
  "circuit_topology_overview": "3-5 sentences identifying the circuit type, describing the overall architecture, and explaining signal flow from input to output.",

  "optimization_variables_mapping": "3-5 sentences for each optimization variable, identifying which transistors it controls and grouping variables by functional role.",

  "optimization_variables_impact": {impact_json_str},

  "variable_interactions": "3-5 sentences describing interactions between optimization variables: which must be scaled together for matching, which have conflicting effects, and which have synergistic effects.",

  "key_insights_for_optimization": [
    "First critical insight about optimizing this circuit (1 sentence)",
    "Second critical insight about optimizing this circuit (1 sentence)",
    "Third critical insight about optimizing this circuit (1 sentence)",
    "Fourth critical insight (optional, 1 sentence)",
    "Fifth critical insight (optional, 1 sentence)"
  ]
}
```
**CRITICAL REQUIREMENTS:**
1. Your entire response MUST be valid JSON - no markdown, no explanations, no text outside the JSON object
2. Do NOT wrap the JSON in code blocks or backticks
3. Each section should be 3-5 sentences focused on OPTIMIZATION VARIABLES
4. The "key_insights_for_optimization" array must contain 3-5 strings (bullet points as array elements)
5. All strings must properly escape special characters (quotes, newlines, etc.)

```

Focus your analysis on the OPTIMIZATION VARIABLES and their impact on performance.

## B.2. Initial Search Space Construction Prompt

### Initial Search Space Construction Prompt

You are an expert analog circuit optimizer. Based on the circuit understanding analysis, your task is to rank all optimization variables by their impact on the target metric and determine the search space.

```

**Circuit Name:** {subckt_name}
**Optimization Target Metric:** {target_metric}
**Number of Variables to Actively Optimize:** {num_variables_to_optimize}
**Total Number of Variables:** {total_num_variables}

**Available Discrete Values:** {variable_ranges}

**Scaling Rules (if applicable):** {scaling_rules}

**Circuit Understanding Analysis:** {circuit_understanding}

**Variable Impact on Metrics:** {variable_impact_summary}

**Variable Interactions:** {variable_interactions}

```

```

**Key Optimization Insights:**
{key_insights}

## Your Task - Part 2: Variable Prioritization and Search Space Configuration

Your task is to:

1. **Rank ALL optimization variables** (1 to {total_num_variables}) based on their
   impact on {target_metric}
2. **Select the top {num_variables_to_optimize} variables** to actively optimize
3. **For the top {num_variables_to_optimize} variables**: Provide sparse search ranges
   covering small to large values (3-7 values each, including extremes)
4. **For the remaining variables**: Determine appropriate fixed values
   (will NOT be optimized)

**Important Considerations:**
- Prioritize variables that have the strongest impact on {target_metric}
- Consider matching requirements and circuit topology
- Balance between search space size and coverage
- Fixed values should enable good performance while allowing optimized variables to
   have maximum impact

### JSON Structure
```json
{
  "optimization_target": "copy target metric here",
  "num_variables_to_optimize": {num_variables_to_optimize},
  "variable_ranking": [
    {
      "rank": <integer>,
      "variable": "<variable_name>",
      "impact_on_target": "<critical/high/medium/low>",
      "reasoning": "<CONCISE explanation max 100 chars - no newlines>"
    }
  ],
  "optimization_configuration": {
    "variables_to_optimize": {
      "<variable_name>": {
        "rank": <integer>,
        "search_space": [<value1>, <value2>, <value3>, ...],
        "num_choices": <integer>,
        "range_reasoning": "<CONCISE max 100 chars - no newlines>",
        "expected_behavior": "<CONCISE max 80 chars - no newlines>",
        "sensitivity": "<high/medium/low>"
      }
    },
    "variables_fixed": {
      "<variable_name>": {
        "rank": <integer>,
        "fixed_value": <numeric_value>,
        "fixed_reasoning": "<CONCISE max 100 chars - no newlines>",
        "why_this_value": "<CONCISE max 80 chars - no newlines>",
        "risk_if_suboptimal": "<low/medium/high>"
      }
    }
  },
  "search_space_summary": {
    "original_full_space": <integer>,
    "pruned_space": <integer>
  }
}
```

```

```

    "reduced_search_space": <integer>,
    "reduction_factor": <number>,
    "calculation": "<mathematical expression>",
    "explanation": "<CONCISE max 100 chars - no newlines>"
  }
}
}

```

### B.3. Optimization Algorithm Orchestration Prompt

#### Optimization Algorithm Orchestration Prompt

ADVANCED SEARCH METHODS AVAILABLE

### Method Arsenal:

```

**1. 'lhs' (Latin Hypercube Sampling)** - Pure Exploration
- **Use when**: Early exploration, design space poorly understood, <10 previous designs
- **Sample size**: Based on search space - larger space needs more samples (15-30% of space, min 15)
- **Parameters**: 'seed' (change each iteration for diversity)

**2. 'genetic' (Genetic Algorithm)** - Evolutionary Exploration
- **Use when**: Want diverse solutions, need robust global search, 10-50 previous designs
- **Sample size**: Based on search space - scales with complexity (10-20% of space, 20-50 samples typical, larger for big spaces)
- **Key Parameters**:
  - 'mutation_rate': 0.2 (normal) → 0.4+ (stuck)
  - 'crossover_rate': 0.8 (default)
  - 'tournament_size': 3

**3. 'bayesian' (Gaussian Process Bayesian)** - Intelligent Exploitation
- **Use when**: 25+ previous results, need sample efficiency, discrete space performance uncertain
- **Sample size**: Based on search space - more samples for larger spaces (5-15% of space, 10-20 samples typical, can go higher for large spaces)
- **Key Parameters**:
  - 'acquisition_function': "EI" (balanced), "LCB" (explore), "UCB" (stuck), "PI" (refine)
  - 'exploration_weight': 0.1-0.3 for EI/PI, 2.0-3.5 for LCB/UCB

**4. 'adaptive' (Multi-Strategy Balance)** - Balanced
- **Use when**: Unsure whether to explore/exploit, want safe balanced approach
- **Sample size**: Based on search space - moderately scales with size (10-20% of space, 15-25 samples typical, adjust for large spaces)
- **Key Parameters**:
  - 'explore_weight': 0.5 (default), 0.6+ (low diversity)
  - 'exploit_weight': 0.5 (default), 0.6+ (late stage)
  - 'random_weight': 0.2 (default), 0.3 (stuck)

**5. 'annealing' (Simulated Annealing)** - Escape Local Optima
- **Use when**: Stuck in plateau, suspect local optimum, need to escape
- **Sample size**: Based on search space - needs more samples for larger spaces (8-15% of space, 12-20 samples typical, scale up for big spaces)
- **Key Parameters**:
  - 'initial_temperature': 2.0 (default), 3.0 (desperate)
  - 'cooling_rate': 0.95

**6. 'multistart' (Multi-Start Local Search)** - Find Alternatives
- **Use when**: Verify convergence, find diverse good designs, late stage
- **Sample size**: Based on search space - more starts for larger spaces (8-15% of space, 12-25 samples typical, proportional to space complexity)

```

```

- **Key Parameters**:
- 'n_starts': 5 (default), 7+ (want diversity or large space)
- 'search_radius': 2

## STRATEGIC DECISION FRAMEWORK

**Diagnose Current Situation:**
- Exploring? → LHS, Genetic, Adaptive
- Exploiting? → Bayesian, Optuna
- Stuck? → Annealing, Multistart
- Converged? → Stop

**Key Factors to Consider:**
1. **Data availability**: <10 designs → LHS/Genetic; 15-25 → Bayesian 30+ → Any method
2. **Improvement trend**: >5% → keep exploring; 1-5% → balance; <1% → exploit or stop
3. **Plateau detection**: 2 iterations no improvement → switch method;
3+ → consider stopping
4. **Search space size**: ALL methods scale with space - larger spaces need more samples

**Parameter Tuning Rules:**
- Stuck/identical designs → increase exploration (higher mutation_rate, exploration_weight, temperature)
- Low diversity (std < 0.01) → increase randomness
- Steady improvement → continue current approach
- Approaching convergence → increase exploitation

## STOPPING RULES
**STOP if:**
1. User specification is met (PRIMARY GOAL)
2. <2% improvement over 2 iterations with diverse methods
3. 3+ iteration plateau with method diversity

**Sample Size Guidelines:**
- **All methods scale with search space size**
- **Exploration methods** (LHS, Genetic, Adaptive): 15-30% of space
- **Exploitation methods** (Bayesian, Optuna, Annealing, Multistart): 5-15% of space
- **LLM Direct**: 5-15% of space (cap individual batches at 20-30 for token limits)
- **General rule**: Larger search space → more samples needed for effective coverage
- **Always**: Cap at remaining budget, consider iteration efficiency

## RESPONSE FORMAT
**CRITICAL - READ THIS CAREFULLY**

### TEMPLATE 1: If you want to CONTINUE optimizing (use "search")
```json
{
  "action": "search",
  "method": "PUT_ALGORITHM_NAME_HERE",
  "n_samples": PUT_NUMBER_HERE,
  "parameters": {
    // Include only relevant parameters for the chosen method
    // For example, if using genetic:
    "mutation_rate": 0.2,
    "crossover_rate": 0.8,
    "tournament_size": 3
    // See method descriptions above for parameter details
  },
  "reasoning": "YOUR_REASONING_HERE",
  "confidence": "high or medium or low",
  "expected_improvement": "YOUR_EXPECTED_IMPROVEMENT",
  "convergence_assessment": "YOUR_CONVERGENCE_ANALYSIS"
}
```

```

```
### TEMPLATE 2: If you want to STOP optimizing (use "stop")
```json
{
  "action": "stop",
  "reasoning": "WHY_STOPPING",
  "confidence": "high or medium or low",
  "expected_improvement": "N/A - converged",
  "convergence_assessment": "CONVERGENCE_EVIDENCE"
}
```

## B.4. Search Space Regeneration Prompt

### Search Space Regeneration Prompt

```
"""You are an expert optimization advisor. RE-EVALUATE and REGENERATE the search space
based on optimization results.

## CONTEXT
After {iterations_completed} iterations with {total_designs} designs evaluated,
re-analyze the circuit and adapt the search strategy.

## CIRCUIT NETLIST (Re-analyze based on actual results)
```
{netlist}
```

**Task:** Re-analyze this circuit considering the optimization results below.
Your previous understanding may have been incorrect.

## ORIGINAL SEARCH SPACE (Your Constraints)

### Available Optimization Variables
**You can ONLY optimize these variables (from YAML config):**
{available_variables}

### Fixed Parameters (CANNOT be changed to variables)
**CRITICAL:** These parameters are PERMANENTLY FIXED and CANNOT be optimized
or unfixed:**
{fixed_parameters}

**WARNING:** DO NOT use any variable names from the "Fixed Parameters" list above in
your optimization_configuration. They are not available for optimization under
any circumstances.**

### Value Ranges (Your choices MUST be subsets of these)
{value_ranges}

**Original Full Search Space:** {original_search_space_size} combinations

## CURRENT CONFIGURATION

### Search Space Comparison
{search_space_comparison}

### Optimized Variables
{optimized_vars_section}

### Fixed Variables
{fixed_vars_section}

**Current Search Space:** {current_search_space} combinations
```

```

## OPTIMIZATION RESULTS

### Performance Progression
{progression_section}

### Convergence Status
- Status: {convergence_status}
- Assessment: {convergence_reason}
- Best FOM: {best_fom}
- Stagnant: {stagnant}

### Variable Impact
{impact_section}

### Issues Detected
{issues_section}

### Top Designs
{top_designs_section}

## YOUR TASK
Decide on action based on the results:
- 'continue_current': Keep current configuration (if performing well and not stagnant)
- 'expand_ranges': Expand variable ranges (preferred if ANY designs at boundaries)
- 'narrow_ranges': Narrow to promising regions (only if very clear winner region)
- 'unfix_variables': Unfix some fixed variables (preferred if stagnation or suboptimal)
- 'change_focus': Swap optimized/fixed variables (if optimized var has low impact)
- 'converged': Optimization complete (only if target met or exhausted search)

## DECISION GUIDELINES

**Expand ranges (PREFERRED ACTION):**
- 20%+ of top designs at boundaries (lowered threshold)
- Current range seems restrictive
- FOM improvements still occurring
- Action: Add 2-3 adjacent values from original ranges on each boundary
- Bias: Favor expansion over narrowing

**Unfix variables (HIGHLY ENCOURAGED):**
- Any fixed variable could impact performance
- Stagnation detected (no improvement for 2+ iterations)
- Current optimized variables explored adequately
- Suspect interactions between fixed and optimized variables
- Action: Unfix 1-2 most promising fixed variables with 5-7 values
- Priority: Unfix before declaring convergence

**Narrow ranges (USE SPARINGLY):**
- Top 80% designs cluster tightly in middle 30% of range
- Very clear single winner region (not just top design)
- Action: Focus on 4-6 best values only
- Warning: Only use if extremely confident

**Change focus (ENCOURAGED FOR EXPLORATION):**
- Optimized variable shows minimal variance in top designs (>70% same value)
- All top designs converged to 1-2 values for a variable
- Action: Fix the converged variable, unfix a new one
- Enables exploring new dimensions

**Continue current:**
- Making steady progress (improvement in last iteration)
- Haven't explored current space adequately (< 40% of combinations)
- No clear issues with current configuration
- Use temporarily, but bias toward taking action

```

```

**Converged (LAST RESORT):**
- Best FOM exceeds or meets target specification
- Improvements < 1% for 4+ consecutive iterations
- All promising variables explored with expanded ranges
- Fixed variables already unfixed and tested
- Warning: Only declare convergence after aggressive exploration

## DECISION PRIORITY ORDER
1. **Unfix variables** - if any fixed variables remain and performance stagnating
2. **Expand ranges** - if any boundary clustering or improvements still occurring
3. **Change focus** - if optimized variable converged but performance suboptimal
4. **Continue current** - if making progress and space not fully explored
5. **Narrow ranges** - only if overwhelming evidence of tight optimal region
6. **Converged** - only after exhausting all exploration options

## CRITICAL CONSTRAINTS
1. **ONLY use variables from "Available Optimization Variables" section above**
2. **Value ranges MUST be subsets of the ranges shown in "Value Ranges" section**
3. **DO NOT create new variables like 'L' if they are fixed parameters**
4. **DO NOT use values outside the allowed ranges**
6. **Each variable: 5-7 discrete values (increased from 3-7 for more exploration)**
7. **Variables in "Fixed Parameters" section CAN be unfixed and optimized**
8. **Bias: When uncertain, choose expansion or unfixing over narrowing or convergence**

## EXPLORATION PHILOSOPHY
- **Default to action**: Prefer exploring (expand/unfix) over staying static
- **Maximize search space**: Unfix variables aggressively before claiming convergence
- **Trust the data**: Only narrow when >80% of evidence supports it
- **Avoid premature convergence**: If in doubt, explore more

## OUTPUT (JSON ONLY)

{{{
  "optimization_target": "{target_metric}",
  "regeneration_reasoning": "<why regenerating>",
  "action_taken": "<action>",
  "changes_from_previous": "<summary of changes>",

  "variable_ranking": [
    {{{
      "rank": <1-n>,
      "variable": "<name>",
      "impact_on_target": "<critical|high|medium|low>",
      "reasoning": "<explanation>"
    }}}
  ],
  "optimization_configuration": {{{{
    "variables_to_optimize": {{{{
      "<variable_name>": {{{{
        "rank": <rank>,
        "search_space": [<values>],
        "num_choices": <number>,
        "range_reasoning": "<why this range>",
        "expected_behavior": "<how target changes>",
        "sensitivity": "<high|medium|low>",
        "change_from_previous": "<what changed>"
      }}}
    }}}},
    "variables_fixed": {{{{
      "<variable_name>": {{{{
        "rank": <rank>,
        "fixed_value": <value>,
      }}}
    }}}
  }}}
}}
```

```

    "fixed_reasoning": "<why fixed>",
    "why_this_value": "<why this value>",
    "risk_if_suboptimal": "<risk>",
    "change_from_previous": "<what changed>"
  } } } }
} } } },
} } } },
"search_space_summary": { {
  "original_full_space": <total>,
  "reduced_search_space": <total>,
  "reduction_factor": "<factor>",
  "change_factor": "<expansion or reduction>",
  "calculation": "<calculation>",
  "explanation": "<explanation>"
} } } },
"expected_improvement": "<expected gain>",
"confidence": "<high|medium|low>"
} } } }

```

Return ONLY JSON based on data.

"""